

## Adlayer Structures of Calixarenes on Au(111) Surface Studied with STM

Ge-Bo Pan,<sup>†</sup> Jian-Hua Bu,<sup>†</sup> Dong Wang,<sup>†</sup> Jun-Min Liu,<sup>†</sup> Li-Jun Wan,\* Qi-Yu Zheng, and Chun-Li Bai\*

Institute of Chemistry, Chinese Academy of Sciences, Beijing 100080, China

Received: May 29, 2003; In Final Form: September 4, 2003

In-situ scanning tunneling microscopy (STM) and cyclic voltammetry have been employed to investigate conformation-related adlayer structures of four calixarenes, three calix[4]arenes with specific conformations and one calix[6]arene. All the molecules form ordered adlayers on the Au(111) surface in 0.1 M HClO<sub>4</sub> under the potential control. For calix[4]arenes, different adlayers are organized on the basis of their specific conformations, indicating that conformations might be used to obtain desired structures. A well-defined adlayer is observed for calix[6]arene. The results demonstrate that the conformation of calixarenes can be immobilized on the Au(111) surface through adsorption, although various conformations of the molecule are reported in solution. The reason is ascribed to the intermolecular and molecule–substrate interactions. On the basis of high-resolution STM images, structural models are tentatively proposed for the ordered adlayers of calixarenes.

## 1. Introduction

Calixarenes, a class of macrocyclic compounds, have attracted much attention because of their unique properties such as conformational flexibility, striking acid–base behavior, and ability to form complexes with a variety of both organic molecules and metal ions.<sup>1,2</sup> In recent years, interest has tremendously increased in the thin films made of calixarenes due to their potentials in microsensors, pyroelectrical devices, and nonlinear optics.<sup>3–7</sup> Various methods such as self-assembly and Langmuir–Blodgett were used to prepare mono- and multilayers of calixarenes. The adlayer structures were further characterized by techniques such as contact angle and grazing angle FTIR.<sup>8</sup>

On the other hand, calixarenes are highly flexible in molecular structures compared with cyclodextrins. Since conformation is important in various reactions and host–guest chemistry, accumulated studies have been carried out to explore the conformational flexibility of calixarenes by experiments (mostly by NMR) and theoretical simulations.<sup>1,2</sup> Results show that the calixarene molecule usually takes various conformations in solution, and a specific conformation can be obtained upon crystallization. To understand the variety of molecular conformations, resolution at the atomic or molecular level is important and is a challenging research activity in calixarene chemistry.

Despite a variety of reports describing the preparation and characterization of ordered adlayers of calixarenes, few direct experimental results were obtained. The adsorption of calixarenes at solid surface and/or electrode/electrolyte interface can be considered as a new approach. The adlayer structures can be directly revealed by STM, which provides detailed information of molecular conformation, orientation, and packing arrangement.<sup>9–11</sup> Recently, we investigated the adsorption of calix[4]arenes on the Au(111) surface by in-situ STM in solution. It is found that different functional groups at the lower or upper rims result in different adlayer structures.<sup>12,13</sup>

Herein, we report conformation-related adlayer structures of four calixarenes (Scheme 1), three calix[4]arenes, and one calix[6]arene. First, the adsorption of calix[4]arenes onto the Au(111) surface is investigated by in-situ STM and cyclic voltammetry. Different adlayers are organized on the basis of their specific conformations. Then, an ordered adlayer of calix[6]arene with various conformations in solution are constructed. Only one adlayer structure is observed in the experiment. On the basis of high-resolution STM images, structural models are tentatively proposed for the ordered adlayers of calixarenes.

## 2. Experimental Section

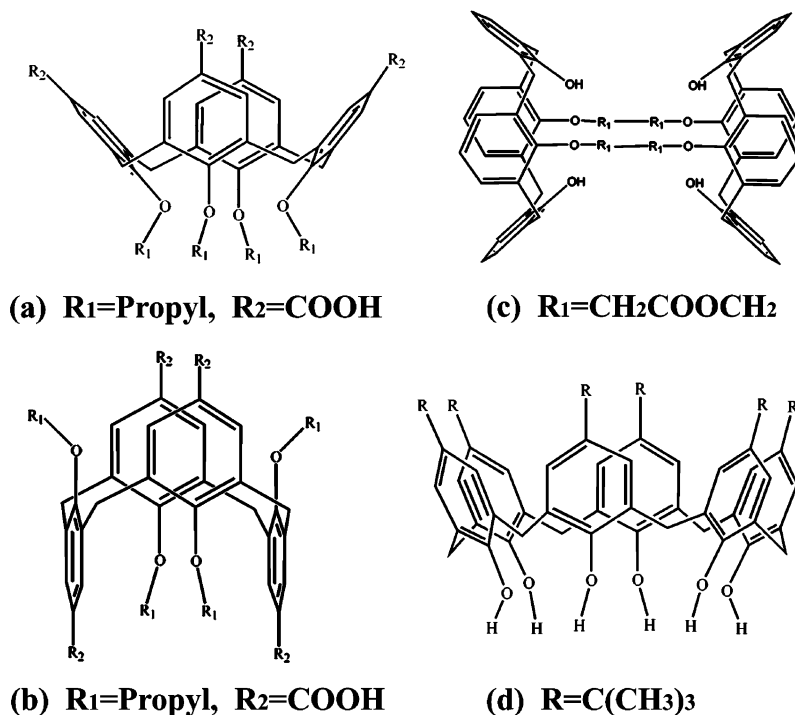
Molecules **a**, **c**, and **d** were synthesized as described in the literature.<sup>14–16</sup> Molecule **b** in the 1,3-alternate conformation was prepared as follows: 1,3-alternate tetrakis(formyl)-calix[4]arene (90 mg) was dissolved in CHCl<sub>3</sub>/acetone (1:1 v/v, 20 mL) and cooled to 0 °C. Aqueous solution (2 mL) of sulfamic acid (147 mg) and sodium chlorite (114 mg) was rapidly added. After 12 h at room temperature, the organic solvents were distilled off and to the residue was added HCl (4 mL). The resulting precipitate was filtered and washed with acetone to obtain the product as a white solid (28 mg, yield 29%). <sup>1</sup>H NMR (DMSO): 0.55~0.68 (m, 12H, CH<sub>3</sub>), 1.17~1.35 (m, 8H, CH<sub>2</sub>-CH<sub>3</sub>), 3.42~3.50 (m, 8H, OCH<sub>2</sub>), 3.84 (s, 8H, ArCH<sub>2</sub>Ar), 7.68 (s, 8H, ArH).

Well-defined Au(111) electrodes were prepared as described previously.<sup>17</sup> An Au(111) facet formed on a single-crystal bead was directly used for the STM experiments. For cyclic voltammetry measurements, one of the (111) facets was mechanically cut, polished by Al<sub>2</sub>O<sub>3</sub> powder, and annealed at 900 °C for 24 h to remove damages on the surface. Before each measurement, the Au(111) electrode was further annealed in a H<sub>2</sub>–O<sub>2</sub> flame and quenched in pure water saturated with H<sub>2</sub>.

Cyclic voltammetry measurements were performed by the so-called hanging meniscus method using an EG&G PAR (Princeton Applied Research) Basic Electrochemical System. A reversible hydrogen electrode (RHE) and a platinum wire were used as reference and counter electrodes, respectively. The solutions were deaerated with high-purity N<sub>2</sub> before experiments

\* Corresponding authors. Fax: +86-10-62558934. E-mail: wanlijun@iccas.ac.cn; clbai@iccas.ac.cn.

<sup>†</sup> Also in Graduate School of Chinese Academy of Sciences, Beijing, China.

SCHEME 1: Chemical Structures of Calix[4]arenes **a**, **b**, and **c**, and Calix[6]arene **d**

were carried out. All the potentials were reported with respect to RHE in 0.1 M  $\text{HClO}_4$ .

In-situ STM experiments were carried out with a Nanoscope E microscope (Digital Instrument Inc., Santa Barbara, CA) in 0.1 M  $\text{HClO}_4$ . The tunneling tip was prepared by electrochemically etching W wire (0.25 mm in diameter) in 0.6 M KOH. The sidewalls of tips were sealed with transparent nail polish to minimize faradaic current. All the images were collected in the constant-current mode to evaluate the corrugation heights of adsorbed calixarenes.

Molecular models of calixarenes were built and optimized by the AM1 method included in HyperChem 6.0 package (Hypercube, Inc.). The interatomic separations and molecular sizes quoted in this study were estimated from these molecular models. Electrolyte solution was prepared with ultrapure  $\text{HClO}_4$  (Kanto Chemical Co., Japan) and Millipore (Milli-Q) water. Saturated solutions of calixarenes were prepared for the STM and electrochemical analysis.

### 3. Results and Discussion

**3.1. Cyclic Voltammetry.** **3.1.1. Calix[4]arenes.** Figure 1 shows cyclic voltammograms (CVs) of an Au(111) electrode in 0.1 M  $\text{HClO}_4$  (dotted line) and 0.1 M  $\text{HClO}_4$  + saturated molecule **a** (solid line) using the so-called hanging meniscus method. It can be seen that the double layer region of bare Au(111) electrode extends from 0 to 1.0 V. When the potential goes more positive, two well-separated characteristic oxidation peaks are found at around 1.3 and 1.5 V as described previously.<sup>18</sup> It is indicated that the surface is a well-defined Au(111) free from the contamination.

After the examination of bare Au(111) electrode, the electrochemical properties of molecule **a** are investigated in 0.1 M  $\text{HClO}_4$  (solid line). No additional peaks are observed in the double layer region, indicating that no redox reaction or structural transformation has occurred. The adsorption of molecule **a** only results in the oxidation peak at 1.3 V in the CV of bare Au(111) electrode to more positive potential region.

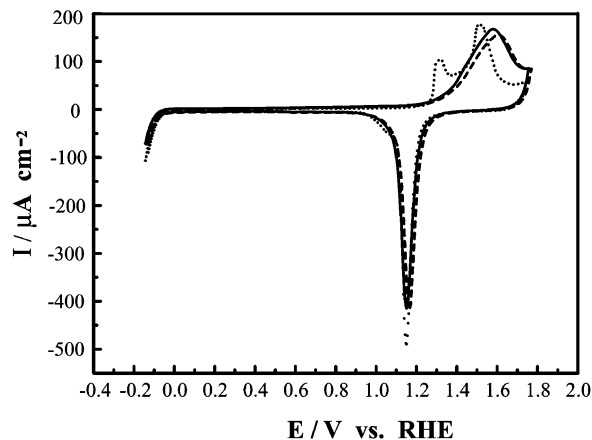


**Figure 1.** Cyclic voltammograms for Au(111) electrode in 0.1 M  $\text{HClO}_4$  (dotted line), 0.1 M  $\text{HClO}_4$  + saturated molecule **a** (solid line), and 0.1 M  $\text{HClO}_4$  + saturated molecule **d** (dashed line). The scan rate was 50 mV/s.

It is suggested that the oxidation of the electrode surface is suppressed due to the adsorption of molecule **a**. Similar results (not shown here) have been obtained for molecules **b** and **c**.

**3.1.2. Calix[6]arene.** Cyclic voltammetry measurement is also carried out to investigate the electrochemical properties of molecule **d** in 0.1 M  $\text{HClO}_4$ , which has various conformations in solution. After recording the standard CV of bare Au(111) electrode (dotted line), a small amount of saturated solution of molecule **d** is directly injected into an electrochemical cell. The overall shape of CV (dashed line) is almost the same as that of Au(111) electrode in the presence of molecules **a**, **b**, and **c**. No additional peaks can be observed in the double layer region. It is suggested that no redox reaction or structural transformation has occurred.

**3.2. In-Situ STM.** **3.2.1. Calix[4]arenes. Molecule a.** A well-defined terrace-step structure is easily observed on the Au(111) surface. Atomic image of Au(111)-(1 × 1) is routinely discerned in the terrace in 0.1 M  $\text{HClO}_4$ . After the examination

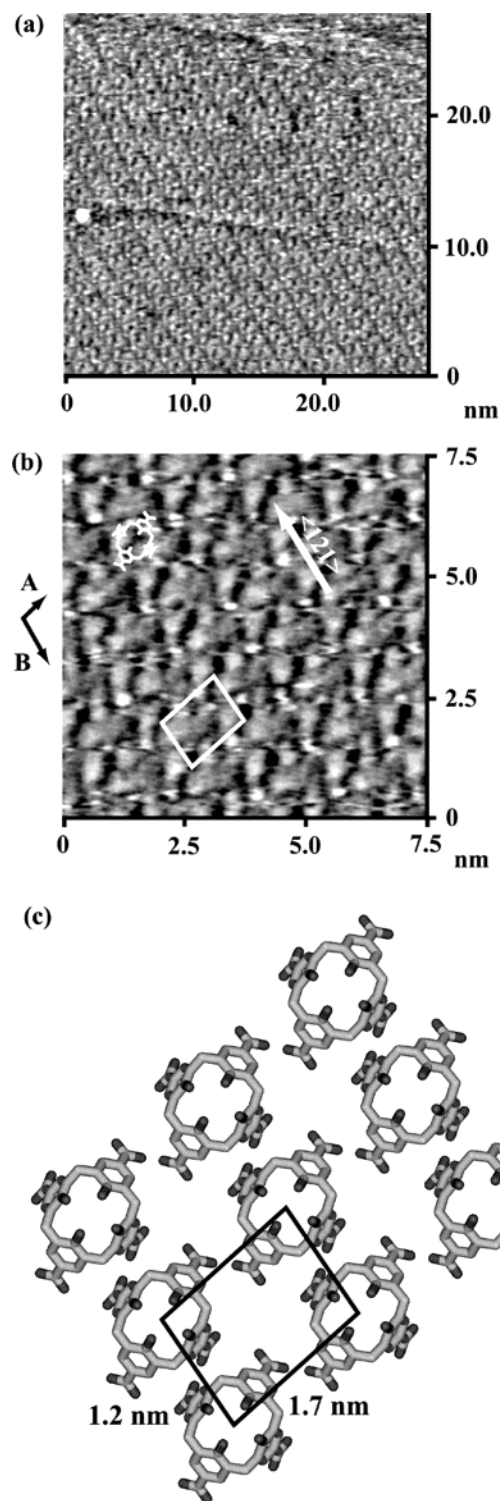
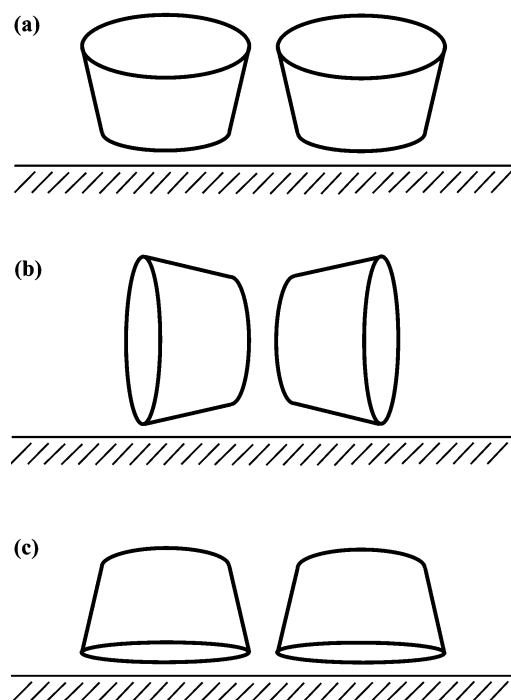


**Figure 2.** (a) Large scale STM image ( $27.3 \times 27.3 \text{ nm}^2$ ), (b) high-resolution STM image ( $7.5 \times 7.5 \text{ nm}^2$ ), and (c) structural model of ordered adlayer of molecule **a** on Au(111) surface in 0.1 M  $\text{HClO}_4$ . The white arrow shows  $\sqrt{3}$  direction determined by the crystallographic orientation of the Au(111) electrode.

of bare Au(111) surface by in-situ STM, a small amount of saturated solution of molecule **a** is directly injected into an STM cell under the potential control of ca. 0.3 V. The concentration of molecule **a** in 0.1 M  $\text{HClO}_4$  is ca.  $1 \times 10^{-6}$  M. Figure 2a shows a typical large-scale STM image of molecule **a** acquired at ca. 0.3 V approximately half an hour later. It is evident that an atomically flat terrace of Au(111) is now covered by an

**SCHEME 2: Schematic Illustration of Three Possible Adsorption Structures of Molecule a on Au(111) Surface: (a) Adsorbed via the Lower Rim, (b) Adsorbed via the Lateral Phenyl Units, and (c) Adsorbed via the Upper Rim**



ordered adlayer of molecule **a**. Despite a relatively large area, each molecule can be recognized as an elliptical protrusion in Figure 2a.

Figure 2b shows a higher resolution STM image obtained in the ordered adlayer, revealing details of internal molecular structure, orientation, and packing arrangement. Obviously, each molecule appears as a rhombus in the STM image. Four bright spots seem to correspond to the phenyl units. The distances between the centers of two bright spots are measured diagonally to be  $6.5$  and  $11.0 \pm 0.2 \text{ \AA}$ , which compare favorably to the size of molecule **a** within the experimental error. Chemical structure suggests that there are mainly three possible structures of molecule **a** adsorbed onto the Au(111) surface (Scheme 2). Schemes 2a and 2c can be used to explain the high-resolution STM image. Considering the existence of carboxyls at the upper rim and propyls at the lower rim, we conclude that molecule **a** is uprightly adsorbed on the Au(111) surface through carboxyl–gold interactions. However, it is difficult to determine the orientation of propyls due to the technical limitation of STM. Thus, no propyls have been illustrated in the structural model. Such policy has also been applied for molecule **b**.

The nearest distances between the two molecules along the **A** direction is  $17 \pm 0.2 \text{ \AA}$ , and  $12 \pm 0.2 \text{ \AA}$  along the **B** direction (Figure 2b). The two vectors cross each other at an angle of  $100 \pm 2^\circ$ . A unit cell is superimposed in the image. Each unit includes one molecule. On the basis of the results described above, a structural model of ordered adlayer of molecule **a** is tentatively constructed as shown in Figure 2c, consistent with a high-resolution STM image (Figure 2b). According to the structural model, the distances and angle do not bear a simple relationship to the corresponding substrate vector within the experimental error in the present investigation. Hence, the parallelogrammic adlayer is incommensurate with respect to the Au(111) lattice. The reason might be attributed to the balance between the intermolecular and molecule–substrate interactions.



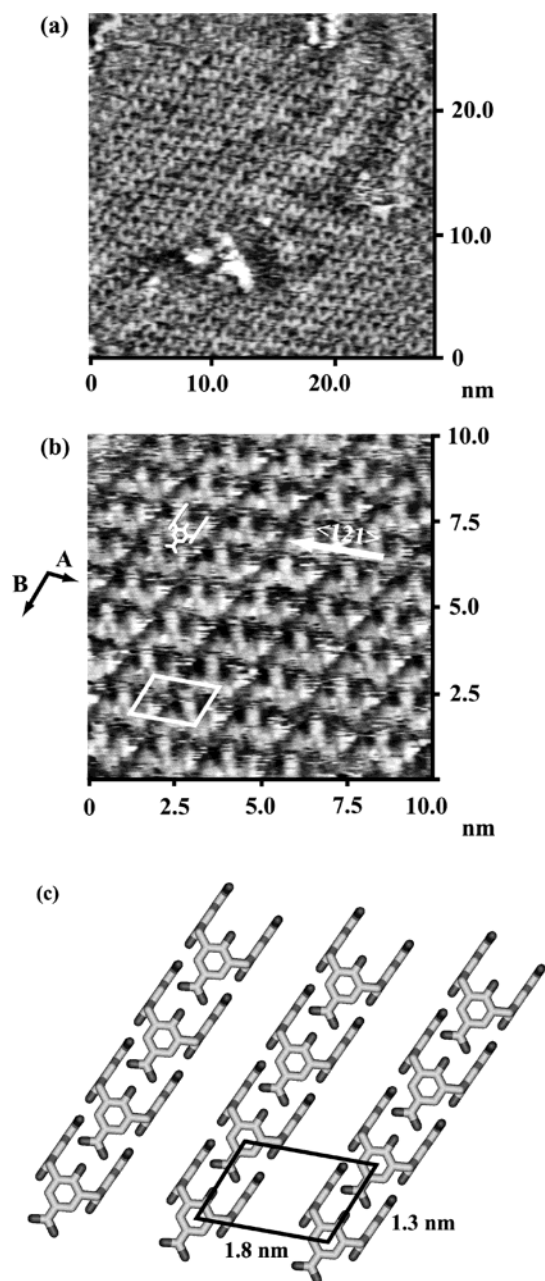


**Figure 3.** (a) Large scale STM image ( $28.0 \times 28.0 \text{ nm}^2$ ), (b) high-resolution STM image ( $10.0 \times 10.0 \text{ nm}^2$ ), and (c) structural model of ordered adlayer of molecule **b** on Au(111) surface in 0.1 M  $\text{HClO}_4$ . The white arrow shows  $\sqrt{3}$  direction determined by the crystallographic orientation of the Au(111) electrode.

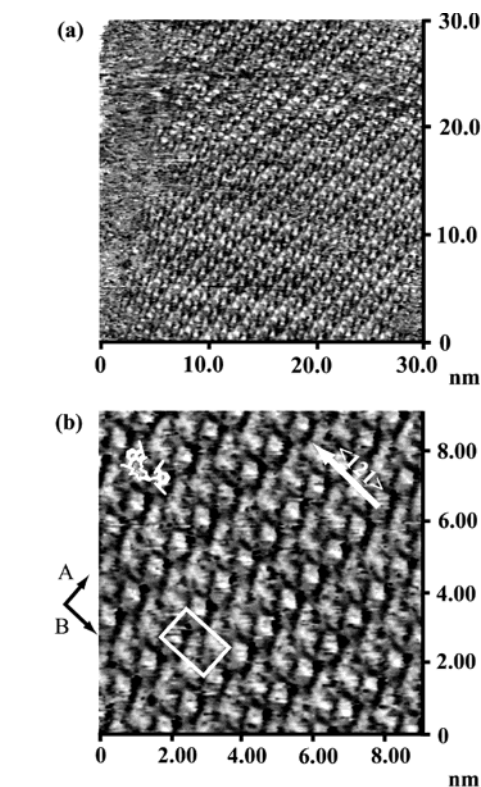
**Molecule b.** Figure 3a shows a typical large-scale STM image of molecule **b** acquired at 0.5 V, which adopts a 1,3-alternate conformation and can be compared with molecule **a** in cone conformation. Despite a relatively large area, each molecule can be recognized as an arc-shaped protrusion in the STM image. Such a feature is significantly different from that of molecule **a** in a rhombus, indicating that different orientations might be taken by molecules **a** and **b**. Figure 3b shows additional details of molecular orientation and packing arrangement of molecule **b** in the ordered adlayer. It is now clear that the protrusion is composed of several bright spots, which can be attributed to the phenyls and propyls. Compared with chemical structure, it can be concluded that molecule **b** is laterally adsorbed on the Au(111) surface through phenyl–gold interactions, which is similar to calix[4]arene.<sup>12</sup> The nearest distances between the

two molecules along the **A** direction are  $18 \pm 0.2 \text{ \AA}$ , and  $13 \pm 0.2 \text{ \AA}$  along the **B** direction. The two vectors cross each other at an angle of  $120 \pm 2^\circ$ , revealing that all the molecular rows are aligned along the  $\sqrt{3}$  direction of the Au(111) electrode. On the basis of the above results, a structural model is constructed for the ordered adlayer of molecule **b** (Figure 3c). The parallelogrammic adlayer is incommensurate with respect to the Au(111) lattice for its lack of simple correlation with the underlying Au(111) lattice.

The above result is really different from that of molecule **a**, which is uprightly adsorbed on the Au(111) surface through carboxyl–gold interactions. From the chemical structure, molecule **b** can also be uprightly adsorbed on the Au(111) surface like molecule **a**. As a result, each molecule should appear as a set of two or four bright spots contributed from the phenyl groups in the STM images acquired with different bias voltages. Nevertheless, this is not the case for molecule **b** in the present experiment. It is indicated that different conformations have resulted in different molecular orientation. Compared with molecule **a**, the carboxyl–gold interactions have been reduced by the propyls for molecule **b**. The hydrogen-bonds between the two neighboring molecules play important roles in forming ordered adlayers. Thus, molecules **b** have self-assembled into rodlike nanostructures. The results show that molecular conformations can be used to obtain desired molecular structures.

**Molecule c.** As a comparison, the adlayer structure of molecule **c**, double calix[4]arene, is briefly investigated on the Au(111) surface in 0.1 M  $\text{HClO}_4$ . Two calix[4]arene units in molecule **c** adopt cone conformation by chemical synthesis and can be compared with molecule **a**. Figure 4a and 4b show typical STM images of molecule **c** acquired at ca. 0.3 V. Each molecule appears as a set of bright spots in the STM image and forms a highly ordered adlayer, which extends over a large area of Au(111) terrace. The nearest distances between the two neighboring molecules along the **A** direction (Figure 4b) is  $11 \pm 0.2 \text{ \AA}$ , and  $18 \pm 0.2 \text{ \AA}$  along the **B** direction. The two vectors cross each other at an angle of  $90 \pm 2^\circ$ . The rectangular adlayer is incommensurate with respect to the Au(111) lattice. Previous studies suggest that laterally adsorbed calix[4]arene appears as one bright spot in the STM images.<sup>12,19</sup> In this case, the separate bright spot may be attributed to one calix[4]arene moiety and the other two bright spots can be assigned as the left moiety included in molecule **c**. On the basis of the above analysis, the structural model has been tentatively constructed as shown in Figure 4c. The structural model is consistent with the observed ordered adlayer of molecule **c**. However, the exact relationship between molecule **c** and the underlying Au(111) lattice could not be determined in the present study as well as molecules **a**, **b**, and **d**. More straightforward experimental techniques such as IR and theoretical calculation must be applied to obtain further structural information to support the above result as well as molecules **a**, **b**, and **d**.

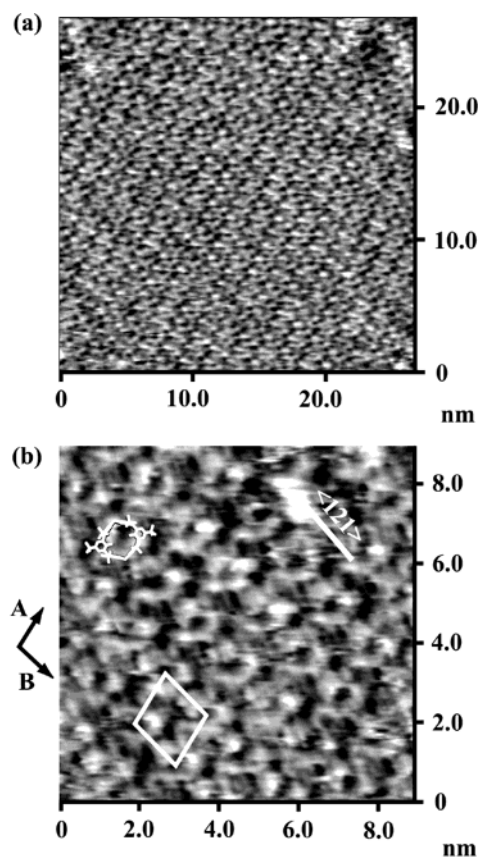
After recording the STM images at 0.3 V shown in Figure 4, the electrode potential is scanned in the increment of 10 mV in the potential region of 0 to 1.0 V. The almost identical adlayer is consistently observed for molecule **c**. It is demonstrated that no structural transformation has occurred. The result is in good agreement with that of cyclic voltammetry. In addition, the ordered adlayer seems to be thermodynamically stable, because such adlayer with certain domain sizes are consistently observed for a long time. Similar results have been obtained for molecules **a**, **b**, and **d**, which suggests that the adlayers are independent of the electrode potential in the range from 0 to 1.0 V.



(c)

**Figure 4.** (a) Large scale STM image ( $30.0 \times 30.0 \text{ nm}^2$ ), (b) high-resolution STM image ( $9.1 \times 9.1 \text{ nm}^2$ ), and (c) structural model of ordered adlayer of molecule **c** on Au(111) surface in 0.1 M  $\text{HClO}_4$ . The white arrow shows  $\sqrt{3}$  direction determined by the crystallographic orientation of the Au(111) electrode.

**3.2.2. Calix[6]arene. Molecule d.** The above experimental procedure has also been carried out to investigate the adlayer structure of molecule **d**, a calix[6]arene derivative, on the Au(111) surface in 0.1 M  $\text{HClO}_4$ . Molecule **d** is supposed to possess various conformations in solution and different from molecules **a**, **b**, and **c** with specific conformations. After the examination of bare Au(111) electrode in 0.1 M  $\text{HClO}_4$ , a small drop of saturated solution of molecule **d** is directly injected into the STM cell under the potential control at ca. 0.5 V. The concentration of molecule **d** in 0.1 M  $\text{HClO}_4$  is ca.  $1 \times 10^{-6}$  M. Figure 5a shows a typical large-scale STM image of



(c)

**Figure 5.** (a) Large scale STM image ( $26.7 \times 26.7 \text{ nm}^2$ ), (b) high-resolution STM image ( $8.9 \times 8.9 \text{ nm}^2$ ), and (c) structural model of ordered adlayer of molecule **d** on Au(111) surface in 0.1 M  $\text{HClO}_4$ . The white arrow shows  $\sqrt{3}$  direction determined by the crystallographic orientation of the Au(111) electrode.

molecule **d** acquired at 0.5 V. It is evident that atomically flat terrace of the Au(111) surface is now covered by an ordered adlayer of molecule **d**. Each molecule can be recognized as an elliptical protrusion in the STM image with dark depressions.

Figure 5b is a higher-resolution STM image, which reveals additional details of molecular orientation and packing arrangement in the ordered adlayer. Each molecule appears as a “calix” in the STM image. Compared with the chemical structure, it can be concluded that molecule **d** is uprightly adsorbed on the

Au(111) surface as illustrated in Scheme 2a. The driving force may come from strong hydroxyl–gold interactions as described previously.<sup>13</sup> Hence, the surrounding protrusion appearing in the STM image can be attributed to the six phenyl units. The dark depression can be assigned as the molecular cavity of molecule **d**. The center-to-center distance along the molecular rows is measured to be  $14 \pm 0.2$  Å. The molecular rows cross each other at an angle of  $110 \pm 2^\circ$ . The rhombic adlayer is incommensurate with respect to the Au(111) lattice. Based on the above analysis, a structural model is tentatively constructed as shown in Figure 5c.

Compared with molecules **a**, **b**, and **c**, molecule **d** is more flexible in the molecular structures. Usually, there are various conformations in solution, and one specific structure can be obtained upon crystallization.<sup>1,2</sup> As a transition state, one may expect that different adlayer structures exist for molecule **d** adsorbed onto the Au(111) surface. However, although efforts such as varying the substrate potential and searching for a large area of Au(111) surface have been made, only one adlayer structure is observed for molecule **d** in the present experiment as shown in Figure 5. It is demonstrated that molecule–substrate and intermolecular interactions may play important roles in immobilizing the conformations. This result may also bridge the gap between the conformational transformation in solution and solid. As a comparison, we have also investigated the adlayer structure of another calix[6]arene derivative (not shown here). The selected calix[6]arene is supposed to possess various conformations in solution similar to molecule **d**. Although the adlayer structure is slightly different from that of molecule **d**, which may result from the different functional groups at the lower rim, one adlayer structure has been observed in the experiment.

It is reported in our previous study that calix[4]arene molecules form dimers through hydrogen-bonds between the lower rim hydroxyls.<sup>12,19</sup> From the chemical structures of molecules **a** and **d**, there also exists the possibility to form dimeric structures on the Au(111) surface. Nevertheless, this is not the case for the two molecules. It is demonstrated that the molecule–gold interaction is stronger than hydrogen-bonds formed by hydroxyls or carboxyls. Thus, molecules **a** and **d** are uprightly adsorbed on Au(111) surface. In addition, the ordered adlayers of two molecules usually extend over a large area of Au(111) terraces, and are thermodynamically stable because such ordered adlayers with certain domain sizes are consistently observed for a long time.

#### 4. Conclusion

Using in-situ STM and cyclic voltammetry, adlayer structures of four calixarenes have been investigated. All the molecules

are found to form highly ordered adlayers on the Au(111) surface in 0.1 M HClO<sub>4</sub>. For calix[4]arenes, different adlayers are organized on the basis of their chemical structures and specific conformations. However, only one adlayer structure, corresponding to one conformation, is observed for calix[6]arene possessing various conformations in solution. The results show that molecular conformations could be immobilized on the electrode surface through adsorption. The reason could be ascribed to the intermolecular and molecule–substrate interactions. Such special properties can be used to obtain desired adlayer structures.

**Acknowledgment.** Financial supports from National Natural Science Foundation of China (Nos. 20025308 & 20177025), National Key Project on Basic Research (Grants G2000077501 & 2000078100), and Chinese Academy of Sciences are gratefully acknowledged.

#### References and Notes

- (1) Gutsche, C. D. *Calixarenes*; Royal Society of Chemistry: Cambridge, 1989.
- (2) Gutsche, C. D. *Calixarenes Revisited*; Royal Society of Chemistry: Cambridge, 1998.
- (3) Schierbaum, K. D.; Weiss, T.; Vanvelzen, E. U. T.; Engbersen, J. F. J.; Reinhoudt, D. N.; Gopel, W. *Science* **1994**, *265*, 1413–1415.
- (4) Kelderman, E.; Derhaeg, L.; Heesink, G. J. T.; Verboom, W.; Engbersen, J. F. J.; Vanhulst, N. F.; Persoons, A.; Reinhoudt, D. N. *Angew. Chem., Int. Ed. Engl.* **1992**, *31*, 1075–1077.
- (5) Richardson, T.; Greenwood, M. B.; Davis, F.; Stirling, C. J. M. *Langmuir* **1995**, *11*, 4623–4625.
- (6) Nabok, A. V.; Richardson, T.; Davis, F.; Stirling, C. J. M. *Langmuir* **1997**, *13*, 3198–3201.
- (7) Chaabane, R. B.; Gamoudi, M.; Guillaud, G.; Jouve, C.; Gaillard, F.; Lamartine, R. *Synth. Met.* **1994**, *66*, 49–64.
- (8) Mandolini, L.; Ungaro, R. *Calixarenes in Action*; Imperial College Press: London, 2000.
- (9) *Adsorption of Molecules at Metal Electrodes*; Lipkowsky, J., Ross, P. N., Eds.; VCH Publishers: New York, 1992.
- (10) Itaya, K. *Prog. Surf. Sci.* **1998**, *58*, 121–247.
- (11) Kolb, D. M. *Surf. Sci.* **2002**, *500*, 722–740.
- (12) Pan, G.-B.; Wan, L.-J.; Zheng, Q.-Y.; Bai, C.-L.; Itaya, K. *Chem. Phys. Lett.* **2002**, *359*, 83–88.
- (13) Pan, G.-B.; Wan, L.-J.; Zheng, Q.-Y.; Bai, C.-L. *Chem. Phys. Lett.* **2003**, *367*, 711–716.
- (14) Sansone, F.; Barbosa, S.; Casnati, A.; Fabbi, M.; Pochini, A.; Uguzzoli, F.; Ungaro, R. *Eur. J. Org. Chem.* **1998**, 897–905.
- (15) Zheng, Q.-Y.; Chen, C.-F.; Huang, Z.-T. *Chin. Chem. Lett.* **2000**, *11*, 403–404.
- (16) Gutsche, C. D.; Dhawan, B.; No, K. H.; Muthukrishnan, R. *J. Am. Chem. Soc.* **1981**, *103*, 3782–3792.
- (17) Wan, L.-J.; Terashima, M.; Noda, H.; Osawa, M. *J. Phys. Chem. B* **2000**, *104*, 3563–3569.
- (18) Angerstein-Kozłowska, H.; Conway, B. E.; Hamelin, A.; Stojcovic, L. *J. Electroanal. Chem.* **1987**, *228*, 429–453.
- (19) Sakai, T.; Ohira, A.; Sakata, M.; Hirayama, C.; Kunitake, M. *Chem. Lett.* **2001**, 782–783.